ELSEVIER

Nuclear Instruments and Methods in Physics Research A 495 (2002) 161–169

NUCLEAR INSTRUMENTS & METHODS IN PHYSICS RESEARCH Section A

www.elsevier.com/locate/nima

A novel detection system for laser cooling of ortho-positronium

Nagendra Nath Mondal*

Department of Physics, Tokyo Metropolitan University, 1-1 Minami Ohsawa, Hachioji-shi, Tokyo 192-0397, Japan

Received 15 February 2002; received in revised form 2 August 2002; accepted 5 August 2002

Abstract

We report on the development of a position-sensitive scintillation detector system for viewing laser-cooled ortho-positronium (oPs) annihilation points. Ortho-positronium can be cooled down to a recoil limit of 0.1 K by an ultraviolet laser in spite of its relatively short lifetime. In order to perform this experiment the wavelength of Cr:LiSAF laser is considered to be 243 nm which corresponds to the transition energy of 1S–2P states of oPs. Thermal positronium plays an important role in laser cooling of oPs. We investigated various kinds and sizes of inorganic scintillators. Position resolutions of YAP:Ce and CsI(Tl), respectively, were determined to be 3.00 and 3.8 mm. Extensive Monte Carlo simulation studies were performed to view the decay positions of oPs using the time-of-flight method. Related issues of position resolution measurements and oPs decaying points will be discussed.
© 2002 Elsevier Science B.V. All rights reserved.

PACS: 36.10D; 55.55.L

Keywords: PSPMT; Scintillator; Positronium; Laser; Monte Carlo

1. Introduction

Positronium (Ps) is the bound state of an electron (e^-) and its antiparticle, the positron (e^+). It is simply an atom without a nucleus, and is one of a family of leptonic hydrogen like systems, which includes muonium (μ^+e^-), tauonium (τ^+e^-) as well as one of a family of more exotic particle–antiparticle systems such as muium ($\mu^+\mu^-$), and protonium. Its energy levels can be explained to a high degree of accuracy by electromagnetic interaction, affording an ideal test of the quantum electrodynamics (QED) theory of bound systems. Laser cooling of ortho-Positronium (oPs) is the first proof-of-principle experiment towards realization of Ps Bose–Einstein Condensation (PsBEC) [1]. Recently, Bose–Einstein Condensation (BEC) of various atoms Rb [2], Na [3], Li [4], etc. was achieved. BEC is increasingly of interest in many other areas of science. Ps is a unique, well-defined exotic atom and hence the BEC of Ps elucidates fundamental aspects of atomic and molecular physics as well as nano-technology. In spite of having a shorter lifetime (142 ns) than ordinary atoms produced at room temperature, it can be cooled down to a recoil limit of 0.1 K by ultraviolet laser. The wavelength (λ) of the Cr:LiSAF laser system is selected to be 243 nm,

*Tel.: +81-426-77-2500; fax: +81-426-77-2483.
E-mail address: mondal@hakone.phys.metro-u.ac.jp (N.N. Mondal).

0168-9002/02/$ - see front matter © 2002 Elsevier Science B.V. All rights reserved.
PII: S0168-9002(02)01578-4

and that λ corresponds to the transition energy of 1S–2P states of Ps. According to the spin–spin interactions, two types of Ps with different lifetimes can be formed on the material surface: oPs, a spin triplet state whose decay modes are odd multiple of γ-rays (3γ, 5γ, 7γ, …,) and para-Ps (pPs), a spin singlet state which has a lifetime of 125 ps and whose decay modes are even multiple of γ-rays (2γ, 4γ, 6γ, …,). Para-Ps could not be the subject of a laser cooling experiment due to its shorter lifetime than the 1S–2P transition times of oPs. The development of a position-sensitive scintillation detector system for viewing the laser-cooled oPs annihilation points is crucial for achieving a variety of future goals in high-energy physics and astrophysics. In order to get better detection efficiency, time and position resolutions than the conventional time-of-flight (TOF) spectrometer [5], we are planning to develop a high-quality position-sensitive scintillation detector system. Using different scintillators of various thickness we optimized the size of the YAP:Ce scintillator, which is a suitable candidate for this measurement technique. To make a complete set of detectors a YAP:Ce is coupled with position-sensitive multianode photomultiplier tubes (PSPMT) by optical glue. The PSPMT provides a very attractive approach to fabricating large, moderately priced position-sensitive arrays with good imaging performance. The basic idea of the laser-cooled oPs detection system is shown in Fig. 1.

In the figure three position-sensitive detectors are radially placed perpendicular to the e^+ beam axis. When low energy e^+ is incident on a clean metal surface, thermalization process occurs immediately inside the material and thermalized e^+ diffuse back towards the surface. Ps work function of the material is negative and that can be formed by e^+ when thermalized e^+ picks up an e^- from the surface. The kinetic energy of this Ps is of the order of a few eV (work function Ps). On the other hand, thermalized e^+ may be trapped inside the surface potential well, form Ps with the near surface e^-, and come out from the surface at an elevated temperature, which is called thermal Ps.

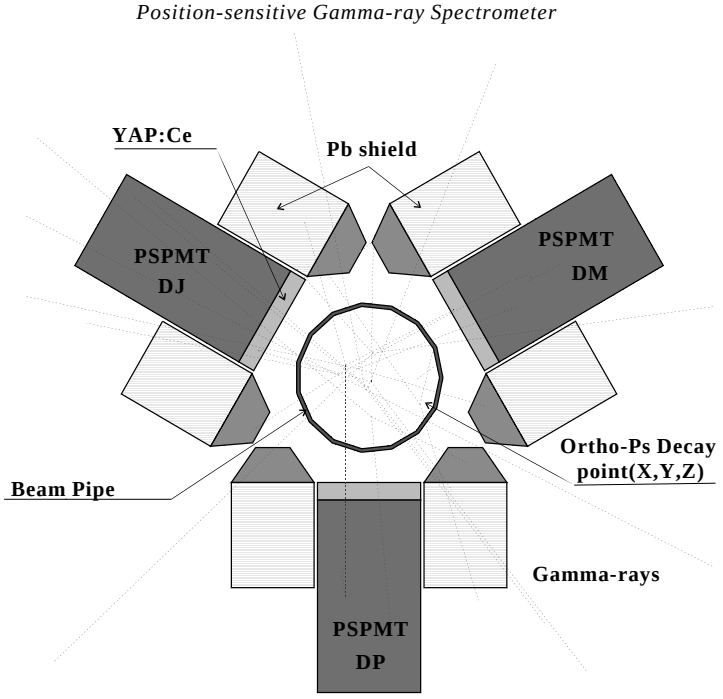

Fig. 1. Basic idea of laser-cooled oPs detection system. Three PSPMT are radially placed perpendicular to the e^+ beam axis 120° apart from each other. This spectrum is designed by Monte Carlo simulation based on GEANT.

The kinetic energy of thermal Ps depends on the temperature of the target, typically a few meV at room temperature and plays a key role in the laser-cooling process. Inside the laser-cooling chamber a heated target will be bombarded by a pulsed e^+ beam in time with pulsed laser, and annihilation γ-rays of oPs will be detected by the TOF method. The thermal Ps production rate is very low (10–20%) in comparison to the work function Ps (50–60%) at room temperature produced on the clean metal surface [6] by slow positron bombardment. In order to separate thermal Ps from the work function Ps, precise time and position resolutions of the measurement apparatus are required. It is difficult to show a sharp TOF peak of thermal Ps using more than 5 mm position resolution of our existing TOF spectrometer and time resolution of pulsed e^+ beam more than 24 ns [7]. We also noticed that thermal Ps detection efficiency became lower if we improved the position resolution towards 5–1 mm and time resolution towards 24–2 ns. One of our main interests is to view the decaying points of laser-cooled oPs within the position resolution less than 5 mm. In the subsequent sections laser cooling of oPs, position resolution measurement, and construction of a position-sensitive detector system will be illustrated.

2. Laser cooling of ortho-positronium

A Ps has two spin states distinguishable by their respective lifetimes and their motions can be optically controlled. Laser cooling has much in common with the field of optics. In laser cooling, light is used to manipulate atoms. Chu et al. measured the 1^3S_1–2^3S_1 interval in Ps via Doppler-free two-photon spectroscopy in 1984 [8]. In their experiment Ps was excited to the 2^3S_1 state by two counterpropagating 486 nm laser pulses. Atoms in the $n = 2$ state were ionized with high probability by the intense laser beams and detected the positrons from the ionization events. They recorded count rate versus laser frequency as the laser was tuned through the 1^3S_1–2^3S_1 resonance. On the other hand, Ziock et al. reported optical saturation of the 1^3S–2^3P transitions in Ps using ultraviolet light from a frequency-doubled, pulsed dye laser in 1989 [9]. They were able to repeatedly excite the Ps atoms in their laser beam to the $n = 2$ levels. They had achieved saturation intensities in a bandwidth which included a significant fraction of Doppler profile and width a maximum transition rate about three times optical saturation. As a first step towards the goal of achieving Ps BEC we have been pursuing an experiment on laser cooling of oPs utilizing the 1S–2P transitions [10]. Our laser cooling system consists of an e^+ beam generator, a TOF spectrometer and a Cr:LiSAF laser. The transition energy of the 1S–2P state of Ps is 5.1 eV and the corresponding wavelength is 243 nm. The wavelength of the Cr:LiSAF laser system is maintained in an ultraviolet region to achieve the same wavelength of the transition energy. When an oPs absorbs a laser photon of frequency ν which has the same energy of the respective states, it will be excited and stay in the 2P state for a while. The amount of absorption will depend on the number of oPs in the 1S state and the density of the radiation. During the spontaneous emission process excited oPs will regress to the 1S state by emitting a photon of the same ν. The spontaneous transition rate is 3.1×10^8/s which corresponds to the lifetime of the 2P state of oPs, i.e., $\tau_{2P} = 3.2$ ns. Therefore, a spontaneous emission process occurs every 6.4 ns, which is twice the lifetime of the 2P state. Needless to say, the decay rate of the 1S state to 3γ-rays decreases due to the direct decay time from the 2P state to 2γ rays (100 μs) is much longer than that from the 2P state; in other words the oPs lifetime is doubled to 284 ns. In the absorption and emission process of a single photon, the oPs obtains a recoil velocity, $v_r = \hbar k/m_{Ps} = 1.5 \times 10^3$ m/s at room temperature. The corresponding energy change can be related to a temperature, the recoil limit, defined as

$$k_B T_r \equiv \frac{\hbar^2 k^2}{m_{Ps}} \tag{1}$$

and T_r is regarded as the lower limit for optical cooling processes. The parameter k is the photon propagation number, k_B is Boltzmann's constant, $\hbar$ is Planck's constant divided by 2π, and m_{Ps} is the mass of Ps which is extremely small $\sim 1.022\,\mathrm{MeV}/c^2$. It should be pointed out that the

one-photon recoil limit (0.1 K) is higher than the Doppler limit (7.5 mK), because of the large recoil energy owing to the small mass of Ps. The typical kinetic energy of thermal Ps is ~ 39 meV at room temperature and the corresponding one dimensional velocity is 4.8×10^4 m/s, so that the cooling cycle is estimated to be $4.8 \times 10^4/1.5 \times 10^3 = 32$ within the recoil limit, thus giving rise to the total cooling time of 200 ns. Using the one-dimensional velocity, the laser line width is required to be 39 pm.

3. Measurement of position resolutions

Results on position resolution measurements carried out by many other groups are listed in Table 1. A review of the literature regarding position resolution measurements and physical properties of the scintillators can be found in Ref. [11] and in the references mentioned there.

A single block and a segmented CsI(Tl) scintillator coupled to a PSPMT have been tested for achieving good position resolution and γ-ray detection efficiency. In order to construct a detector, a PSPMT (Hamamatsu Photonics Co., H6568) of 4×4 cells (effective surface area of each cell $4.5\,\text{mm} \times 4.5\,\text{mm}$) is coupled with a CsI(Tl) crystal of size $30\,\text{mm} \times 30\text{mm} \times 5\,\text{mm}$ by optical glue. To measure the e^+e^- free annihilation γ-rays produced in the ^{22}Na source, we set another NaI(Tl) scintillator of size $(50\varphi \times 30)\,\text{mm}^3$ coupling with a PMT detector directly opposite to the PSPMT detector. Electronic readout of this measurement system is illustrated in Fig. 2.

During the data acquisition process we have seen that pulses produced at PSPMT have shorter time widths than that of the PMT detector. We used a sixteen-channel Shaper amplifier for integrating the signals into wider time width. Signals obtained by all cells of PSPMT are linearly summed by a linear mixer and obtained by an ADC-1. Using the same ADC we obtained energy detected by PMT. A sixteen-channel PH ADC-2 is used to obtain energy responses from each cell of the PSPMT detector. To generate gates of ADCs we synchronized the two detector's output by setting appropriate discriminator threshold levels, fixed delay and time windows on each side; explicitly making the trigger of the measurement. The x- and y-positions are reconstructed (arbitrary unit, a.u.) by the following equations:

$$x = \frac{\sum_{i=1}^{16} a_i E_i}{E_{\text{tot}}} \tag{2}$$

and

$$y = \frac{\sum_{i=1}^{16} b_i E_i}{E_{\text{tot}}} \tag{3}$$

where a_i and b_i, respectively are the ith cell positions in two dimensions and E_i is the corresponding energy observed by the respective cell, and

$$E_{\text{tot}} = \sum_{i=1}^{16} E_i$$

is the total energy summed over 16 cells. During the data analysis we made a two-dimensional scatter plots of energies obtained by ADC-1. The energy

Table 1
Progress on the position resolution measurements

Group name	Year	Crystals (mm^3)	PSPMT	Energy (keV)	Position res. (mm)	Energy res. (%)
1. Uchida et al.	1986	BGO ($5 \times 5 \times 20$)	—	511	5.0	—
2. Nagai et al.	1994	GSO ($50\varphi \times 5$)	R2486	511	2.2	—
3. Nagai et al.	1996	BGO ($2.2 \times 2.2 \times 15$)	R3941	511	2.7	—
4. Mondal et al.	2000	YAP:Ce ($30\varphi \times 1$)	H6568	59	2.2	24
5. Mondal et al.	2001	BGO ($30 \times 30 \times 20$)	H6568	511	17.0	24
6. Mondal et al.	2001	CsI(Tl) ($30 \times 30 \times 5$)	H6568	511	3.8	18
7. Mondal et al.	2001	CsI(Tl) ($4.5 \times 4.5 \times 30$)	H6568	511	5.7	24
8. Mondal et al.	2001	YAP:Ce($30 \times 30 \times 5$)	H6568	511	3.0	12
9. Mondal et al.	2001	YAP:Ce($30 \times 30 \times 5$)	H6568	59	3.3	21

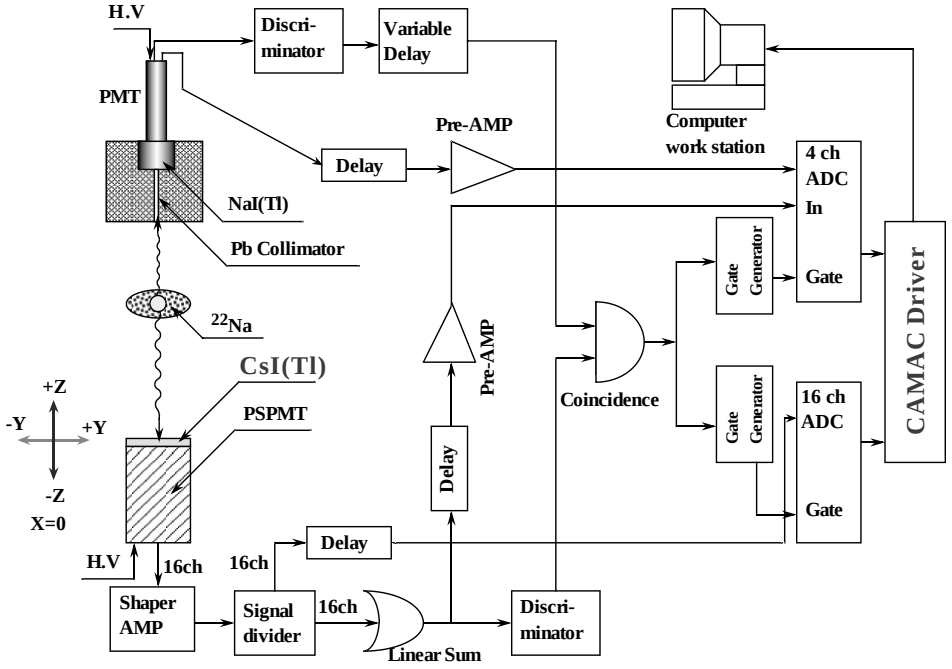

Fig. 2. An electronic readout of position resolution measurement is schematically shown. Data is taken by on-line computer network system and analyzed using Physics Analysis Tools PAW.

spectra obtained by the two detectors are displayed, respectively in Fig. 3(a) and (b). The two-dimensional scattered plot is shown in Fig. 3(c).

We selected events from the scattered plot around 511 keV (hatch marks in (a) and (b)) peaks and made reconstruction using Eq. (2) and Eq. (3). When we took the data of the x-positions, the y-position of the detector was kept fixed and vice versa. In Fig. 4(a), the reconstructed $\pm x$ positions are displayed. The flat tail of each spectrum is attributed to background originating from the detected Compton γ-rays by neighboring cells of the online cell hit by the 511 keV. The peak positions of each spectrum is fitted with a Gaussian distributions and extrapolated. After normalization with the central spectrum X-2, all extrapolated data are shown in Fig. 4(c). Out of eight sets of data, four are presented in Fig. 4(a) for clarity. The marks X-1, X-2 and so on at (c) correspond to those of (a). The width of the central spectrum is much wider than that at the edges and gradually becomes narrower when the γ-ray hits closer the edge of the scintillator. In a similar manner we have reconstructed the y-position.

All the mean values of the Gaussian fitted data of the x-position distribution are plotted on the vertical axis and the corresponding geometrical positions in the horizontal scale, which is shown in Fig. 4(b). The data points are approximately linear from –8 to 4 mm and then saturated near the edge attributing to the small effective surface area (44%) of the PSPMT. The data points are fitted with a polynomial function for determining the conversion factor (α), a parameter (slope of the fitted line) that can be used to convert a.u. to a real scale in mm. The resolution η is determined by the following equation:

$$\eta_{\mathrm{FWHM}} = \frac{2.35 \times \sigma_{\mathrm{av}}}{\alpha} \tag{4}$$

where

$$\sigma_{\mathrm{av}} = \sum_{i=1}^{N} \sigma_i / N$$

an average sigma value and N is the number of data. An average position resolution of this scintillator is determined from the measurements

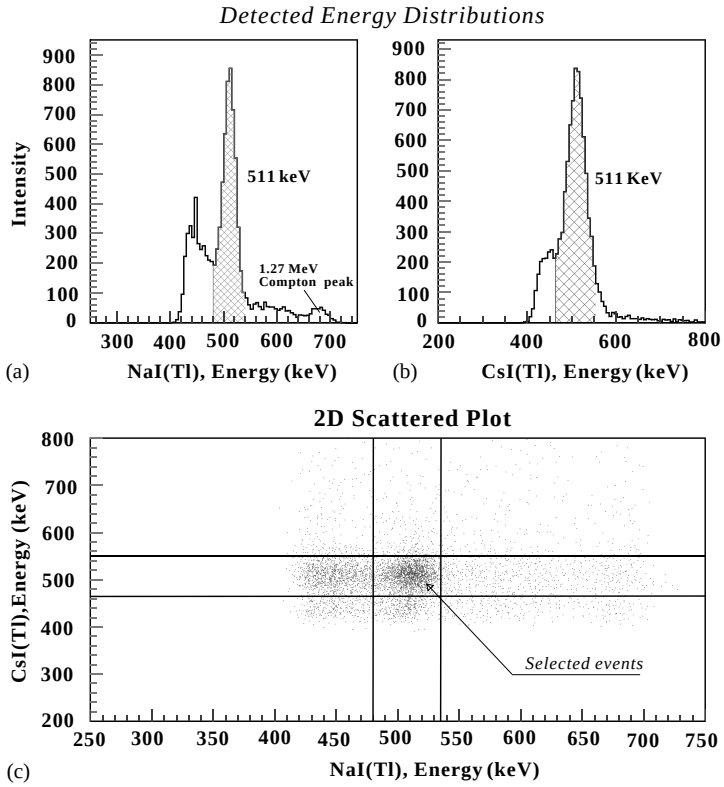

Fig. 3. Energy distributions obtained by two detectors are displayed, respectively in (a) and (b). Events are selected from the two-dimensional scattered plot, which is shown in (c), and selected energy regions are indicated by hatch marks in (a) and (b), respectively.

of the x- and y-positions, which is to be 3.85 mm at FWHM. Using the same technique of the CsI(Tl) scintillator block we investigated YAP:Ce of the same size and determined the position resolution 3.0 mm at FWHM with lower γ-ray detection efficiency [11]. To increase the detection efficiency we designed a CsI(Tl) crystal of size $4.5\,\text{mm} \times 4.5\,\text{mm} \times 30\,\text{mm}$ pixel with 2D array (4×4 cells). Each cell is optically separated from the others. Crystal cells are well matched with the cells of PSPMT and coupled as before. Using the similar technique of position resolution measurement (see Fig. 2) we accumulate data and a typical spectrum of 4 cells along the $\pm x$-axis (2nd row from the top) is presented in Fig. 5. Events are selected around 511 keV peaks from the scattered plot between cells of PSPMT and PMT detectors.

The selected event numbers of 511 keV are plotted along the vertical axis and corresponding geometrical positions of PSPMT on the horizontal scale. Spectra of cell-6 and cell-7 show Gaussian distributions. On the other hand, spectra of cell-5 and cell-8 are half-Gaussian, because there are no other extra cells beyond these two cells. An average position resolution is determined to be 5.7 mm at FWHM from the Gaussian fitted standard deviations.

4. Construction of a position-sensitive detector and image reconstruction

PSPMT coupled to a thin scintillator such as CsI(Tl) or YAP:Ce is an attractive approach achieving good spatial and energy resolutions. In order to construct a position-sensitive γ-ray spectrometer and reconstruct an image of the decaying points of oPs, an extensive Monte Carlo simulation based on GEANT [12] is performed. A

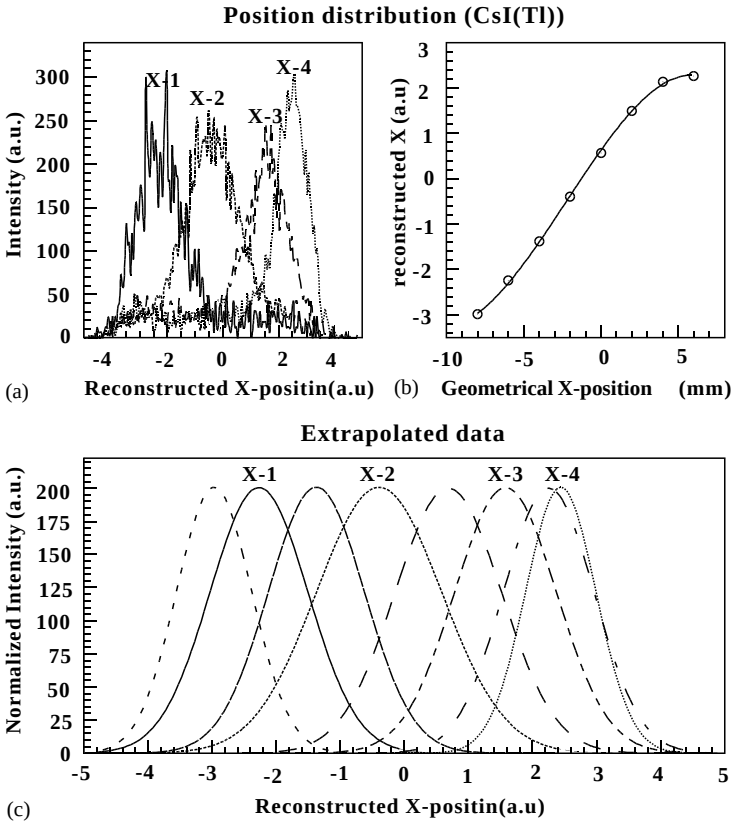

Fig. 4. Reconstructed x-position (a.u.) distributions of γ-rays in each position of the PSPMT: (a) shows the real data, (b) reconstructed mean x-positions (a.u) obtained from those data of (a), and plotted with respective geometrical positions of PSPMT, (c) extrapolated data obtained from (a).

YAP:Ce scintillator is coupled with a PSPMT of 16 cells, and a set of three detectors is radially placed perpendicular to the e^+ beam axis 120° apart from each other (see Fig. 1). This idea of the oPs detection system is unique and we have been developing this spectrometer to support our laser cooling of oPs experiment. In the simulation codes several assumptions, and real parameters of the detectors, are introduced. We generated thermal Ps at room temperature, and 6 mm beyond the center of the spectrometer. Thermal Ps follows the Maxwell–Boltzmann distribution and we consider its distribution on the target surface to be Gaussian. Ortho- and para- Ps are generated 3:1 with their respective lifetimes. Utilizing the GRACE-BASES/SPRING files 3γ-rays are generated. We synchronized the three detectors and the threshold energy was set to be 200 keV. This amount of energy cut was good enough to reduce the normal background and the Compton scattering effects in the experiment. To view the decay points of oPs we have performed a computational image reconstruction method using Monte Carlo simulation [11]. In Fig. 6, a view of reconstructed oPs decaying points is illustrated, where energy and momentum conservations of detected 3γ-rays are taken into account. We assume that conservation takes place in the laboratory reference frame, Ps is the lightest atom and thermal energy is extremely smaller than the annihilation γ-ray energies. The detection efficiency of thermal oPs is determined to be 10^{-4}%.

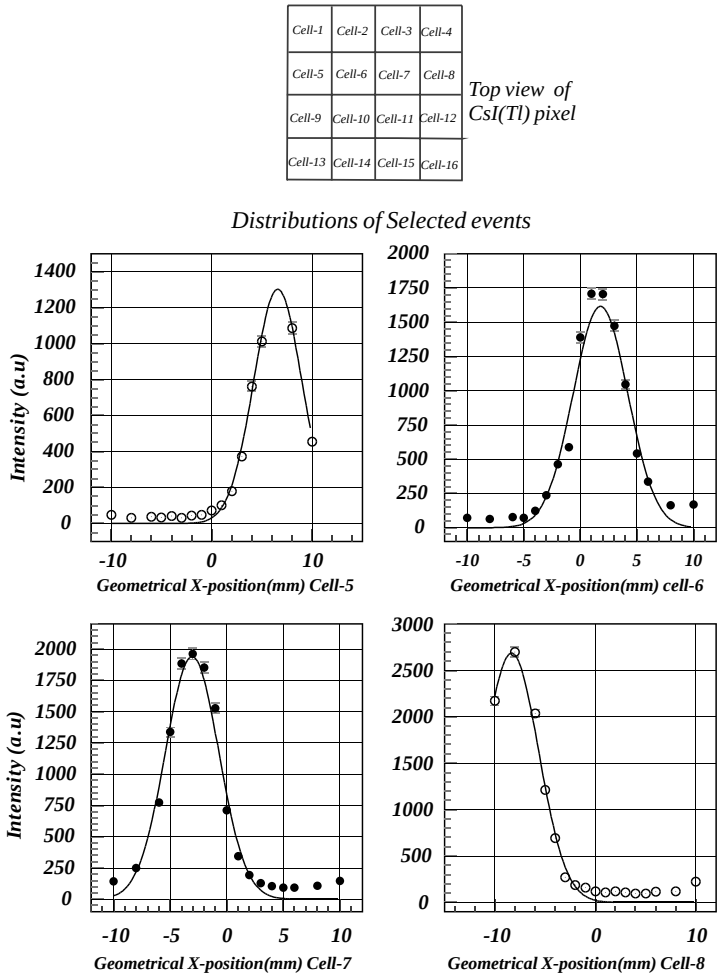

Fig. 5. Selected 511 keV events are plotted on the vertical axis with corresponding PSPMT position (mm). PSPMT positions are moved along the x-axis (2nd row of scintillator array, shown on the top of the spectrum, for details see text).

5. Discussions and conclusion

We have investigated different inorganic scintillators of various sizes. The aim of these extensive investigations is to achieve better position resolution and detection efficiency (see Table 1). In a particular energy measurement detection efficiency is proportional to the scintillator thickness, i.e., thicker scintillator gives better detection efficiency. Other properties of scintillation materials such as γ-ray attenuation length, light yield, etc. are also important factors for achieving better detection efficiency. PSPMT is another crucial factor for determining the detection efficiency, energy and position resolutions. It can be mentioned that a thinner scintillator shows better position resolution than a thicker one and that can be seen from the tabulated results. Position resolution does not depend on the incident γ-ray energy, but strongly depends on scintillator thickness. A YAP:Ce scintillator was recently developed and might be a good candidate for our experimental purpose due to higher light output than BGO, shorter decay time than CsI(Tl), and excellent stopping power. On the other hand, light yield of YAP:Ce is very stable in comparison to other scintillators up to several hundred degree Kelvin temperatures, and which is a non-hygroscopic. Thermal Ps

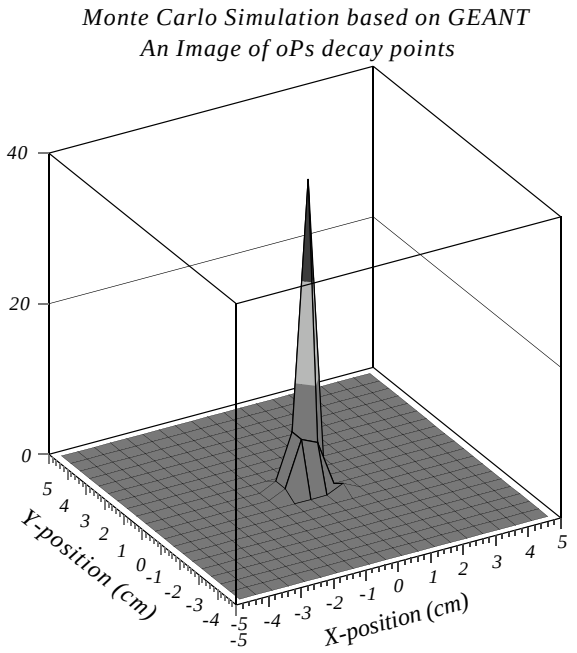

Fig. 6. A two-dimensional view of oPs annihilation points is shown, which is performed by computational image reconstruction algorithms.

production rate is maximized at the highest temperature (~ 1000 K) of the target. In the laser cooling experiment e^+ beam is magnetically guided onto the target surface by solenoid coils (SC) surrounding the beam pipe and Helmholtz coils. Higher temperature might be produced near the detectors' area because of SC for a long-term experiment. If we set position-sensitive detectors very close to the SC in order to increase the detection efficiency, YAP:Ce scintillator appears to be the best choice.

YAP:Ce shows better energy resolution resulting in better position resolution in comparison with other scintillators. Energy resolutions of some other scintillators are shown in Table 1. It might be possible to improve our spatial resolution using the smaller dinode size PSPMT (8×8 or 16×16 cells) and this is under consideration. There is a current trend of achieving 511 keV energy resolution <10–12%, spatial resolution <5 mm in the Positron Emission Tomography (PET) cameras. Our results may play a key role in designing modern PET and Compton Gamma Cameras. Thermal Ps and laser cooling of oPs experiments are in progress. The critical density of observing BEC state of Ps is about $\sim 1.8 \times 10^{16}$ atoms/cm^3 [1], and it seems that this system is a vital candidate for making an image of Bose condensate of rare-decay experiment within a finite position resolution.

Acknowledgements

I would like to thank Prof. R. Hamatsu and Prof. T. Hirose for encouraging this project and for useful discussions and Prof. Martin Guest for a critical reading of the manuscript. I gratefully acknowledge a fellowship award from Japan Society for the Promotion of Science (JSPS).

References

[1] T. Hirose, H. Iijima, M. Irako, M. Kajita, K. Kobayashi, T. Kumita, N.N. Mondal, K. Wada, H. Yabu, Proceedings of the International Conference on LASERS, Albuqueque, NM 2000, p. 437.
[2] M.H. Anderson, et al., Science 269 (1995) 198.
[3] K.B. Davis et al, Phys. Rev. Lett. 75 (1995) 3969.
[4] C.C. Bradley, C.A. Sackett, R.G. Hulet, Phys. Rev. Lett. 78 (1997) 985.
[5] N.N. Mondal, R. Hamatsu, T. Hirose, H. Iijima, M. Irako, T. Kumita, Y. Igura, T. Omori, Appl. Surf. Sci. 149 (1999) 269.
[6] A.P. Mills Jr., E.D. Shaw, M. Laventhal, R.J. Chichester, D.M. Zuckerman, Phys. Rev. B 44 (1991) 5791.
[7] K. Wada, T. Asonuma, T. Hirose, H. Iijima, M. Irako, K. Kadoya, T. Kumita, B. Matsumoto, N.N. Mondal, H. Yabu, K. Kobayashi, M. Kajita, ICFA-2001 Proceeding, June 11–17, in press.
[8] S. Chu, A.P. Mills Jr., J.L. Hall, Phys. Rev. Lett. 52 (1984) 1689.
[9] K.P. Ziock, C.D. Dermar, R.H. Howell, F. Magnotta, K.M. Jones, J. Phys. B 23 (1990) 329.
[10] T. Hirose, T. Asonuma, H. Iijima, M. Irako, K. Kadoya, T. Kumita, B. Matsumoto, N.N. Mondal, K. Wada, H. Yabu, 18th Advanced ICFA Beam Dynamics Workshop on Quantum Aspects of Beam Dynamics, Capri, October 15–20, 2000.
[11] N.N. Mondal, T. Hirose, Appl. Surf. Sci. 194 (1–4) (2002) 317–324.
[12] GEANT—Detector Description and Simulation Tool, CERN Program Library, CERN, Geneva, Switzerland.